Single-step Replacement of an Unreactive C-H Bond by a C-S Bond Using Polysulfide as the Direct Sulfur Source in the Anaerobic Ergothioneine Biosynthesis

Ronghai Cheng,[†1] Lian Wu,[†2, 8, 9] Rui Lai,[†1] Chao Peng,[†3] Nathchar Naowarojna,[†1] Weiyao Hu,[1,4] Xinhao Li,[4] Stephen A. Whelan,[1] Norman Lee,[1] Juan Lopez,[1] Changming Zhao,[1,5] Youhua Yong,[2] Jiahui Xue,[6] Xuefeng Jiang,[6] Mark W. Grinstaff,[1,7] Zixin Deng,[5] Jiesheng Chen,[4] Qiang Cui,[1*] Jiahai Zhou,[2*] and Pinghua Liu[1*]

ABSTRACT: Ergothioneine, a natural longevity vitamin and antioxidant, is a thiol-histidine derivative. Recently, two types of biosynthetic pathways were reported. In the aerobic ergothioneine biosyntheses, non-heme iron enzymes incorporate a sulfoxide to an sp^2 C-H bond from trimethyl-histidine (hercynine) through oxidation reactions. In contrast, in the anaerobic ergothioneine biosynthetic pathway in a green sulfur bacterium, *Chlorobium limicola,* a rhodanese domain containing protein (EanB) directly replaces this unreactive hercynine C-H bond with a C-S bond. Herein, we demonstrate that polysulfide (HSS_nSR) is the direct sulfur-source in EanB-catalysis. After identifying EanB's substrates, X-ray crystallography of several intermediate states along with mass spectrometry results provide additional mechanistic details for this reaction. Further, quantum mechanics/molecular mechanics (QM/MM) calculations reveal that the protonation of N_π of hercynine by Tyr353 with the assistance of Thr414 is a key activation step for the hercynine sp^2 C-H bond in this trans-sulfuration reaction.

Keywords: ergothioneine biosynthesis; polysulfide; C-H bond activation; transsulfuration; crystal structure.

▪ INTRODUCTION

Sulfur-containing natural products are widely distributed in nature, yet their biosynthetic details are poorly understood.[1-6] One such natural product is ergothioneine, a thiol-histidine derivative (**4**, **Figure 1**). Ergothioneine and glutathione (GSH) are among the most abundant cellular thiols in animals.[7] Together, they maintain a proper redox environment under a wide range of conditions due to their difference in reduction potential (~200 mV).[7,8] Animals enrich ergothioneine from their diet through an ergothioneine-specific transporter (OCTN1) to millimolar concentrations in various parts of the body.[9] Ergothioneine is touted as a longevity vitamin,[10] and many diseases may benefit from ergothioneine treatment, including rheumatoid arthritis, Crohn's disease, diabetes, cardiovascular diseases, and neurodegeneration.[8]

In ergothioneine biosyntheses, the key step is the substitution of the hercynine's ε-carbon sp^2 C-H bond with a C-S bond (**1** to **4** transformations, **Figure 1a**); a remarkable example of C-H bond activation in synthesis.[11-13] In recent years, two types of ergothioneine biosynthetic pathways were discovered: the aerobic and anaerobic biosynthetic pathways. In the aerobic ergothioneine biosynthetic pathways from *Mycobacterium smegmatis*[14] and *Neurospora crassa*[15] (**Figure 1a**), a non-heme iron enzyme (EgtB or Egt1, respectively, **Figure 1a**) catalyzes the hercynine's ε-carbon sp^2 C-H bond activation using molecular oxygen as the oxidant. While in the anaerobic ergothioneine biosynthetic pathway from the green-sulfur bacterium *Chlorobium limicola,* a rhodanese (EanB-catalysis, **Figure 1a**) is proposed to directly replace the sp^2 C-H bond by a C-S bond, using cysteine as the sulfur source and cysteine desulfurase (IscS) as the sulfur-transfer mediator (**Figure 1b**).[16,17] In general, the rhodanese active site's cysteine persulfide intermediate transfers its terminal sulfur atom to an activated acceptor,[18-20] yet, in EanB-catalysis, the hercynine's sp^2 C-H bond is not activated.[16,17] In contrast to the original proposal of cysteine along with IscS as the sulfur source (**Figure 1b**),[16,17] herein, we report the unprecedented finding that polysulfide is the direct sulfur source for EanB-catalysis. In green-sulfur bacteria, the deposited sulfur granules contain several forms of polysulfides, including S_8, polysulfide, cysteine polysulfide, and glutathione polysulfide.[21-23] In this report, we demonstrate that all of these different deposited polysulfides in sulfur bacteria could serve as EanB substrates, suggesting that this reaction is a biologically relevant transformation. Kinetic studies,

mass spectrometry analyses, and X-ray crystal structures of the pre-reaction complex, the reaction intermediate, and the product complex of EanB-catalysis provide additional mechanistic details and insights into this reaction. Further, we propose a mechanistic model for this intriguing trans-sulfuration reaction based on experimental data as well as QM/MM metadynamic simulations. Given the wide-distribution of EanB homologs in nature, the discoveries in this report may serve as the starting point for characterizing many more similar reactions in the biosyntheses of sulfur-containing natural products.

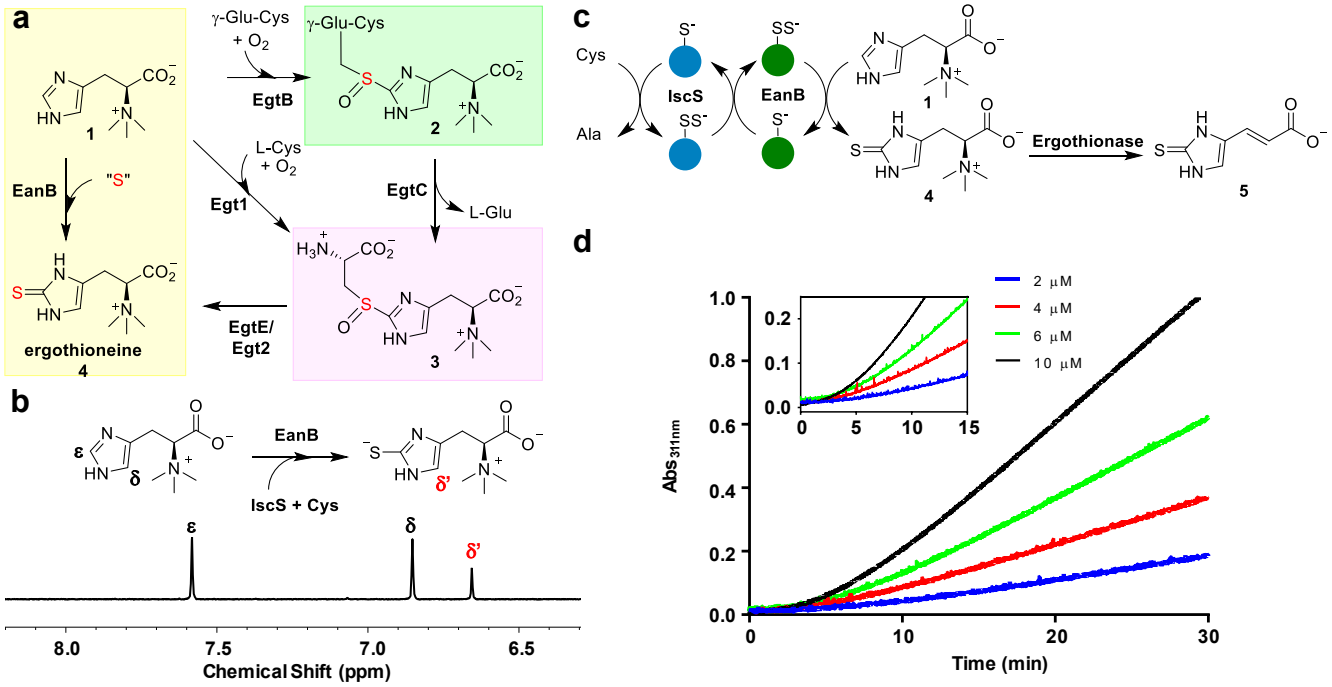

Figure 1. Ergothioneine biosynthesis and our initial EanB characterization. (**a**) Ergothioneine biosynthetic pathways: two aerobic (EgtB-EgtC-EgtE-catalysis in mycobacteria, and Egt1-Egt2-catalysis in fungi), and an anaerobic (EanB-catalysis in sulfur bacteria) pathways. (**b**) ^{1}H-NMR of the IscS-EanB coupled reaction shows ergothioneine production. The ~7.6 ppm and ~ 6.9 ppm signals are from the hydrogen atoms of hercynine's side-chain and the signal at ~ 6.7 ppm is from the ergothioneine's side-chain hydrogen atom. (**c**) The reaction scheme of the IscS-EanB-ergothionase coupled assay, in which the formation of thiourocanic acid **5** is monitored at 311 nm by UV-visible spectroscopy. (**d**) A five-minute lag phase for the IscS-EanB-ergothionase coupled assay. The reaction mixture contained 2 μM IscS, 1 mM cysteine, 1 mM hercynine, 400 nM ergothionase (1000-fold of EanB activity), and EanB at various concentrations (2-10 μM) in 50 mM pH 8.0 potassium phosphate (KPi) buffer at 25 °C. The reaction was monitored at 311 nm ($\varepsilon_{311nm} = 1.8 \times 10^5\ M^{-1}{\cdot}cm^{-1}$).

▪ RESULTS

Lag-phase in EanB-catalysis and the production of elemental sulfur (S_8) in the IscS-EanB coupled reaction. Recently, Seebeck and coworkers reported their biochemical studies of EanB-catalysis from the anaerobic ergothioneine biosynthesis in which cysteine was used as the direct sulfur source and the *Escherichia coli* cysteine desulfurase (IscS) was used as the sulfur transfer mediator (**Figure 1b**).[17] The *E. coli* IscS was used to replace the *C. limicola* IscS for three reasons. First, compared to other cysteine desulfurases,[24-27] IscS is a promiscuous enzyme participating in the biosynthesis of thio-cofactors such as Fe-S clusters, thiamin, and biotin.[28-30] Second, the *E. coli* IscS shares high sequence similarity to that of the *C. limicola* IscS (**Figure S1a**). Finally, the structural model of the *C. limicola* IscS created by us using the Phyre2 program is highly similar to the reported *E. coli* IscS crystal structure (**Figure S1b**).[31]

We first repeated the EanB reaction reported by Seebeck and co-workers.[17] Indeed, the IscS-EanB coupled reaction produces ergothioneine (**Figure 1b**) as revealed by ^{1}H-NMR assay. The ~7.6 ppm and ~ 6.9 ppm signals are from the hydrogen atoms of hercynine's side-chain and the signal at ~ 6.7 ppm is

from the ergothioneine's side-chain hydrogen atom (**Figure 1b**). After demonstrating the EanB-activity, in order to accurately measure the EanB kinetic parameters, we developed a continuous assay (**Figure 1c**). In this assay, we included ergothionase,[32] which degrades ergothioneine to thiolurocanic acid **5**. Because thiolurocanic acid **5** has a strong absorption feature centered at 311 nm (ε_{311nm} = 1.8 × 10^5 M^{-1}•cm^{-1}), we could use this coupled assay to accurately measure the kinetic parameters of EanB-catalysis. Interestingly, when we monitored the thiolurocanic acid formation at 311 nm continuously (the IscS-EanB-ergothionase coupled reaction to form thiolurocanic acid **5**, **Figure 1c**), we noted two interesting observations: First, the formation of thiolurocanic acid (**5**) has a five-minute lag phase (**Figure 1d**). Second, the reaction mixture becomes cloudy after four hours. We collected these precipitates and characterized them. The dominant component in the precipitate is elemental sulfur (S_8), along with a very small amount of the denatured EanB protein (**Figure S1c-f**). In the literature, it has been reported that when IscS is used as the sulfur transfer mediator, if a proper sulfur acceptor is not present, IscS-catalysis will lead to the accumulation of elemental sulfur (S_8).[33,34] Given these literature IscS-examples, the results from our ergothionase coupled assay imply that the Cys-IscS pair may not be the biological sulfur source for EanB-catalysis.

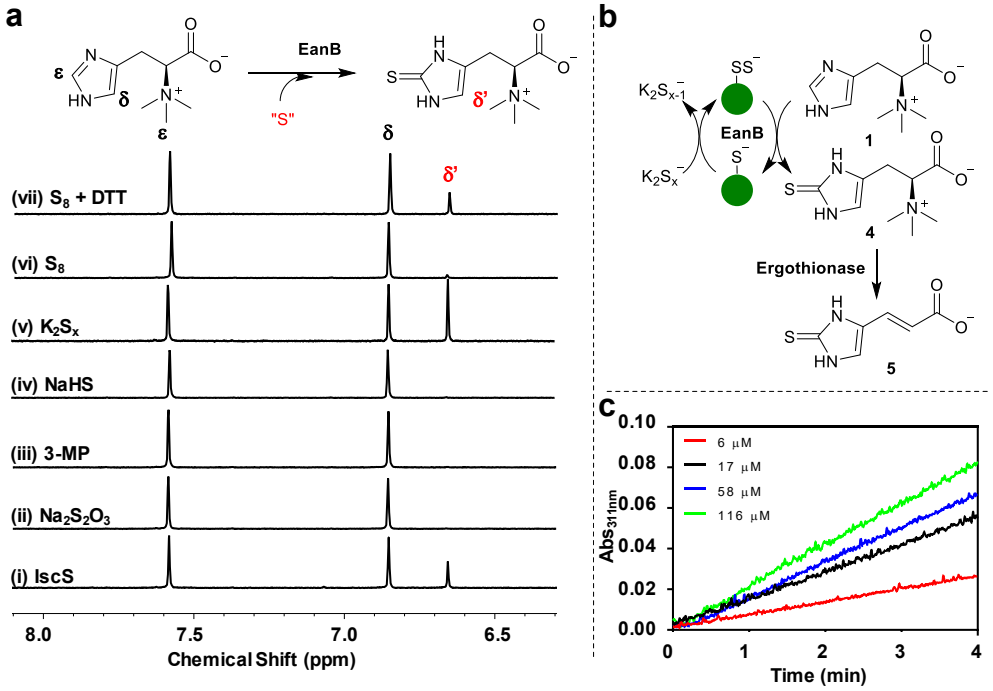

Figure 2. Polysulfide is the direct sulfur source in EanB-catalysis. (**a**) ^{1}H-NMR assay of reaction mixtures using various potential sulfur-donors, including (i) IscS+cysteine, (ii) sodium thiosulfate ($Na_2S_2O_3$), (iii) mercaptopyruvate (3-MP), (iv) sodium bisulfide (NaHS), (v) potassium polysulfide (K_2S_x), (vi) elemental sulfur (S_8), and (vii) dithiothreitol (DTT)-treated elemental sulfur. (**b**) The EanB-ergothionase coupled assay using polysulfide as the direct sulfur source. (**c**) Representative kinetic traces of EanB-polysulfide reactions. The reaction mixture contained 1 mM hercynine, 400 nM ergothionase (1000-fold of EanB activity), and 2 μM EanB and polysulfide at various concentrations (6-116 μM) in 50 mM pH 8.0 KPi buffer at 25 °C. The reaction was monitored at 311 nm (ε_{311nm} = 1.8 × 10^5 M^{-1}•cm^{-1}). There is no lag phase when polysulfide is used as the direct sulfur source.

Polysulfide as the direct sulfur source in EanB-catalysis. Results from our IscS-EanB-ergothionase coupled assay (**Figure 1d** and **Figure S1**) do not support the hypothesis of an IscS-bound persulfide as the direct sulfur source for EanB-catalysis as previously proposed (**Figure 1b**).[17] Therefore, the key question to be addressed in EanB-catalysis is: what are the EanB substrates, especially the identity of its direct sulfur source? To answer this question, we examined several potential sulfur donors for EanB-catalysis (**Figure 2a**), including thiosulfate ($Na_2S_2O_3$), mercaptopyruvate (3-MP), bisulfide (NaHS), and polysulfide.[18,35] Among these sulfur donors, only polysulfide supports robust ergothioneine production (trace v, **Figure 2a**), while the octasulfur ring (S_8) provides a barely detectable level of er-

gothioneine (trace vi, **Figure 2a**). Treatment of S_8 with dithiothreitol (DTT) to produce polysulfide, also affords a significantly enhanced level of ergothioneine (trace vii, **Figure 2a**). More importantly, no lag phase exists in the EanB-ergothionase coupled-assay when polysulfide is the direct sulfur source (**Figure 2c** vs **Figure 1d**). The steady-state kinetic parameters of wild type EanB ($EanB_{WT}$) are: k_{cat} of 0.68 ± 0.01 min^{-1}, K_m of 69.7 ± 8.7 μM for hercynine (**1**), and K_m of 18.1 ± 1.2 μM for polysulfide (**Figure S1g-h**). Polysufides are a mixture of sulfanes with various chain lengths. Following literature protocols,[36] we have characterized the composition of polysulfides in our reaction conditions. The dominant form of polysulfide in our assay conditions is S_4^{2-} (**Figure S2**), therefore, the K_2S_4 concentration was used when we report the K_M of polysulfide.

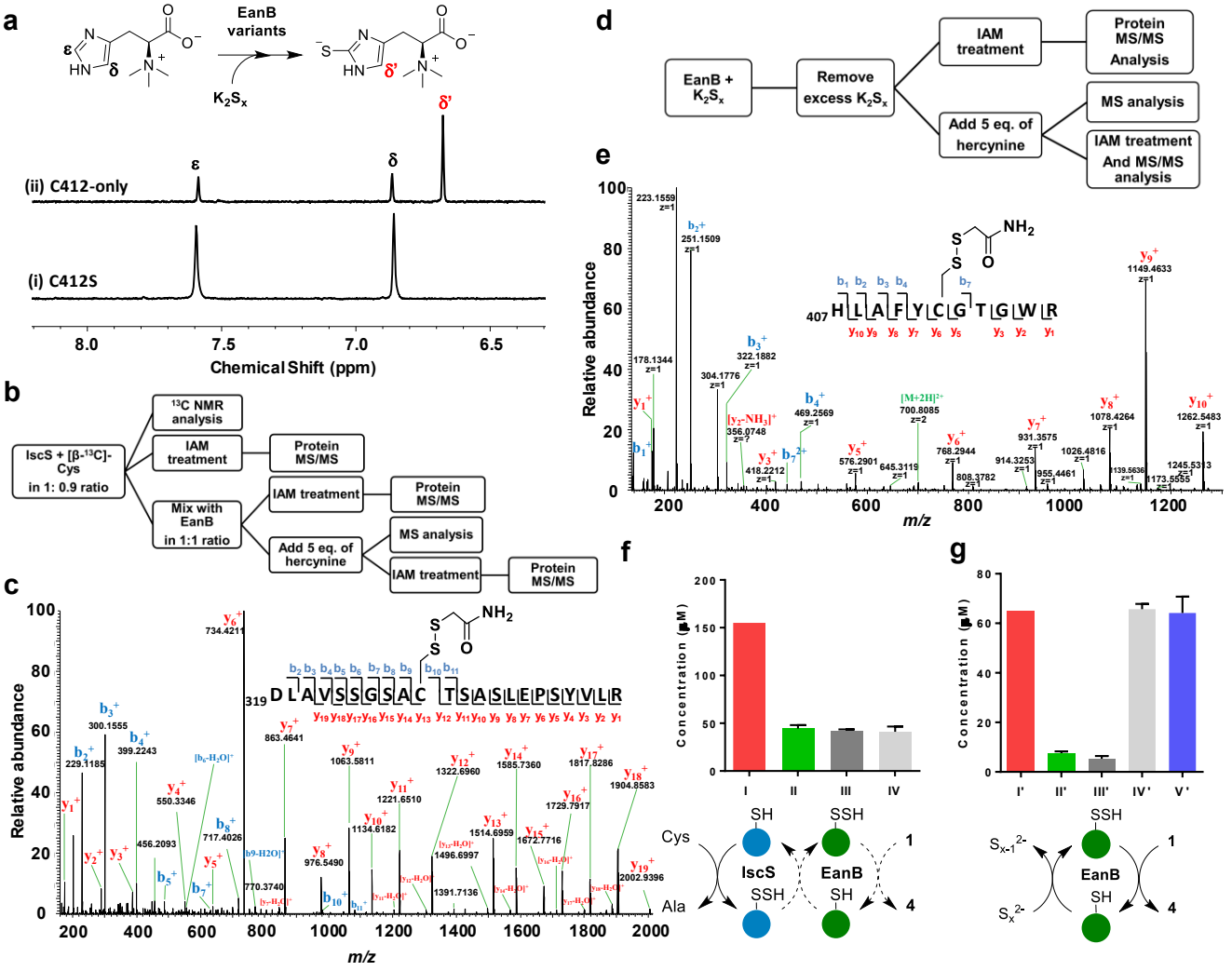

Figure 3. Single-turnover studies to distinguish between the IscS-EanB and EanB-polysulfide reactions. (**a**) ^{1}H-NMR analysis of EanB variants: The $EanB_{C412S}$ reaction (trace i) and $EanB_{C412\text{-}only}$ reaction (trace ii). (**b**) Flowchart of the $EanB_{C412\text{-}only}$ single-turnover reaction using persulfide containing IscS as the direct sulfur source. (**c**) MS/MS analysis of IscS (residues 319 - 340) for detecting the IscS Cys328 persulfide intermediate. (**d**) Flowchart of the $EanB_{C412\text{-}only}$ single-turnover reaction using K_2S_x as the direct sulfur source. (**e**) MS/MS analysis of $EanB_{C412\text{-}only}$ (residues 407 - 417) for detecting the Cys412 persulfide intermediate. (**f**)-(**g**) Quantification of the amount of $EanB_{C412\text{-}only}$ protein (bar I or I'), $EanB_{C412\text{-}only}$ Cys412 persulfide (bar II or II'), ergothioneine produced using as-purified EanB (bar III or III') and ergothioneine produced using IscS- or polysulfide-treated EanB (bar IV or V'). Additionally, quantification of $EanB_{C412\text{-}only}$ Cys412 persulfide after polysulfide treatment is shown in bar IV'.

Cys412 is the only cysteine required for EanB catalysis. There are five cysteine residues in EanB. In literature examples of sulfurtransferases, the sulfur-transfer process may involve multiple cysteine residues.[4] To determine the importance of these five cysteine residues (Cys116, Cys184, Cys339, Cys370, Cys

412), we conducted two sets of experiments. In the first set of experiments, we generated the cysteine to serine mutation for each of the five cysteine residues. The catalytic activities of these mutants were characterized by both ^{1}H-NMR and mass spectrometry. Among them, the $EanB_{C412S}$ mutant is completely inactive. Even under single-turnover conditions, there is no ergothioneine production for the $EanB_{C412S}$ mutant (trace i in **Figure 3a**). Results from the first set of experiments imply that Cys412 might be the active site cysteine residue. In the second set of experiment, we demonstrated that Cys412 is the only required cysteine in EanB-catalysis by creating the $EanB_{C412\text{-}only}$ mutant and characterizing its activity. To create the $EanB_{C412\text{-}only}$ mutant, we replaced all of the other four cysteine resides (Cys116, Cys184, Cys339, and Cys370) with alanine. Therefore, in the $EanB_{C412\text{-}only}$ mutant, there is only one cysteine residue, which is Cys412. Consistent with the hypothesis of having Cys412 as the active site cysteine residue concluded from the first set of experiments, the $EanB_{C412\text{-}only}$ variant is active (trace ii, **Figure 3a and Figure S4b**) and its activity is only a few folds less than that of wild type EanB. The steady state kinetic parameters are: k_{cat} of 0.15 ± 0.01 min^{-1}, K_m of 65.9 ± 3.4 μM for hercynine, and K_m of 10.4 ± 1.0 μM for polysulfide (**Figure S3b-c**). The results from these two sets of studies indicated that Cys412 is the active site's cysteine in EanB and that it is the only cysteine needed for catalysis.

Single-turnover studies to provide further evidence supporting polysulfide as the direct sulfur source in EanB-catalysis. There are two potential mechanistic models to explain the observed ergothioneine production in the reported Cys-IscS-EanB system (**Figure 1b**). In the first model, EanB undergoes a conformational change to expose its Cys412 to the surface, which could then accept a sulfur atom from the persulfide intermediate on cysteine desulfurase (IscS). The second model is proposed based on results from our studies outlined in **Figure 1** & **2**. We proposed that polysulfide, instead of the IscS-persulfide, is the direct sulfur source in EanB-catalysis (**Figure 2a**). In our Cys-IscS-EanB studies, we detected the production of a large amount of elemental sulfur (S_8). The formation of S_8 involves polysulfide intermediates,[33,34] which, therefore, also explains the production of ergothioneine in the Cys-IscS-EanB system (**Figure 1b**) and the presence of a five-minute lag-phase in the kinetics of the Cys-IscS-EanB-ergothionase coupled assay (**Figure 1d**).

To provide further evidence to differentiate between the above two mechanistic options, we conducted two sets of single-turnover studies. In the first set, we prepared persulfide-containing IscS and used the IscS-persulfide as the sulfur source to conduct the EanB single-turnover study (**Figure 3b**). In the second set of experiments, we pre-incubated EanB with polysulfide and after excess polysulfide removal by gel-filtration, polysulfide-treated EanB was then used for the single turnover studies (**Figure 3d**). In addition, to simplify the data analysis, we used the $EanB_{C412\text{-}only}$ variant because Cys412 is the only cysteine residue needed for EanB-catalysis.

In the IscS-$EanB_{C412\text{-}only}$ single turnover study (**Figure 3b**, **3c**, & **3f**), we first incubated IscS with [β-^{13}C]-cysteine in 1:0.9 ratio anaerobically for 5 minutes to produce the IscS-Cys_{328}-persulfide (**Figure S4a**). The formation of the IscS-Cys_{328}-persulfide intermediate is supported by analysis using mass spectrometry. After the IscS-cysteine reaction, the resulting IscS protein was derivatized by iodoacetamide (IAM). The presence of the IscS-Cys_{328}-perfulfide was then characterized by analyzing its alkylated Cys_{328}-based peptide-S-S-acetamide adduct using tandem mass spectrometry (**Figure 3b** and **3c**). Indeed, tandem mass spectrometry analysis of IscS peptides obtained from trypsin-digested IscS supports the production of the IscS-Cys328-persulfide in the IscS-catalyzed cysteine desulfurase reaction (**Figure 3c**).

After the production of Cys_{328}-persulfide containing IscS, it was then mixed with one equivalent of EanB, followed by the addition of an excess amount of hercynine (**Figure 3b**). The amount of ergothioneine produced was quantified via mass spectrometry (**Figure S4c-f**).[15] The amount of the $EanB_{C412\text{-}only}$ Cys412 persulfide content was quantified using cyanolysis according to a literature procedure.[16,37] A typical example of the IscS-$EanB_{C412\text{-}only}$ single-turnover study results are shown in **Figure 3f**. In the as-purified $EanB_{C412\text{-}only}$ (155 μM, bar I), there are 44.4±3.6 μM having Cys412 persulfide modification already (bar II). The amount of ergothioneine produced by mixing the as-purified $EanB_{C412\text{-}only}$ with excess amount of hercynine is 42.0±1.5 μM (bar III). After mixing $EanB_{C412\text{-}only}$ with the Cys328 persulfide containing IscS and then treated with an excess amount of hercynine, the amount of ergothioneine produced is 41.1±5.5 μM (bar IV), which clearly indicates that the Cys328 persulfide containing IscS does not improve the amount of ergothioneine produced by the $EanB_{C412\text{-}only}$ protein under single-turnover conditions. Therefore, results from this single turnover study do not support a direct transfer of the sulfur atom from the

IscS-Cys_{328}-perfulfide to EanB-Cys_{412} to form the EanB-Cys412-persulfide.

In the polysulfide-$EanB_{C412\text{-only}}$ single-turnover studies (**Figure 3d**), the treatment of $EanB_{C412\text{-only}}$ with polysulfide yields the Cys412-persulfide containing $EanB_{C412\text{-only}}$ protein. After the polysulfide treatment, the excess polysulfide was removed by gel filtration and a portion of the polysulfide treated $EanB_{C412\text{-only}}$ was alkylated with IAM and characterized by tandem mass spectrometry, which supports the successful production of the EanB-Cys412-persulfide (**Figure 3e**). The rest of the polysulfide treated $EanB_{C412\text{-only}}$ protein was then mixed with an excess amount of hercynine for the single-turnover study (**Figure 3d**). A typical example of the polysulfide single-turnover experimental result is shown in **Figure 3g**. After the treatment of $EanB_{C412\text{-only}}$ (bar I') with K_2S_x, the amount of Cys412 persulfide increased from 7.7±0.6 μM in the as purified $EanB_{C412\text{-only}}$ protein (bar II') to 65.7±2.2 μM in the K_2S_x treated $EanB_{C412\text{-only}}$ protein (bar IV'). In addition, when the K_2S_x treated $EanB_{C412\text{-only}}$ protein was mixed with an excess amount of hercynine, 64.2±6.6 μM of ergothioneine was produced (bar V'), which is significantly higher than the amount of ergothioneine (5.3±1.1 μM) produced from the as-purified C412-only protein (bar III'). This experiment clearly indicates that polysulfide is the direct sulfur source in EanB-catalysis (**Figure 3g**).

EanB accepts other forms of polysulfides as the sulfur donors. For decades, polysulfides have been known to be present in biological systems and their potential chemical and biological roles are attracting interest.[35,38] The EanB gene was identified from *C. limicola*, which is a green sulfur bacterium. Green sulfur bacteria accumulate sulfur and deposits sulfur globules, with the short length of polysulfides (S_3^{2-} and S_4^{2-}) being the dominant species in the periplasmic space.[21-23] Recently, Prange *et al.* characterized bacterial sulfur granules using X-ray absorption spectroscopy[23] and identified S_8, polysulfide, cysteine polysulfide, and glutathione polysulfide in these sulfur granules. To determine whether other polysulfide forms could support EanB-catalysis, we synthesized glutathione polysulfide and cysteine polysulfide by mixing glutathione or cysteine with the octasulfur ring (S_8) (**Figure S5** and **S6**).[35] In this reaction, the free thiol groups from cysteine and glutathione nucleophilically attack S_8 to produce glutathione and cysteine polysulfide (**Figure S7a**). Using glutathione polysulfide or cysteine polysulfide as the sulfur source, we also observed ergothioneine production (**Figure S7b**). As shown in trace vi of **Figure 2**, when the octasulfur ring (S_8) is used as the substrate in EanB-catalysis, there is a very low level of ergothioneine production. Some of EanB's non-essential cysteine residues are solvent exposed and they might react with octasulfur ring (S_8) to produce a small amount of linear polysulfide to support EanB-catalysis. The green sulfur bacteria accumulate sulfur and deposit sulfur globules in the periplasmic space. However, EanB is predicted to be a cytosolic protein based on the sequence analysis from PSLpred and CELLO.[39,40] Therefore, the cytosolic pool of polysulfide are the ones relevant to EanB-catalysis. Future studies will focus on characterizing this cytosolic pool of polysulfides.

Snapshots of several EanB-catalysis intermediate states. After establishing polysulfide as the direct sulfur source for EanB-catalysis (**Figure 2 & 3**), we solved EanB X-ray structures in several states using polysulfide as the substrate. The structures of EanB alone and its complex with hercynine were reported recently by Leisinger *et al.*[16] and are consistent with our results (**Table S1, Figure S8**, and **S9**). In contrast to other literature rhodanese examples, whose active site's cysteine residues are surface exposed (**Figure S9a-b**), the EanB active site Cys412 reside at the bottom of a ~13 Å deep tunnel (**Figure S9c**). This unique EanB structural feature is consistent with our discovery of polysulfide as the direct sulfur source because polysulfide could access the deeply buried Cys412, while the IscS-Cys328 may not.

In continuation of our mechanistic studies, we captured three additional states of EanB-catalysis by X-ray crystallography (**Figure 4a-4c**). Upon co-crystallization of EanB with polysulfide and hercynine, we observed an EanB•hercynine binary complex with the Cys412 persulfide (**Figure 4a** & **Figure S10a**). In this structure, the distance between the Cys412 persulfide's terminal sulfur and hercynine's ε-carbon is 3.2 Å (**Figure 4a**), which is longer than a C-S bond (~1.82 Å). The dihedral angle between the Cys412-persulfide and the hercynine's imidazole ring is -141.8°. Therefore, this structure is most likely the EanB•hercynine•persulfide intermediate before the sulfur-transfer reaction (the pre-reaction state). In the EanB pre-reaction state (**Figure 4a**), Tyr353 is 3.1 Å away from the hercynine's ε-carbon, suggesting its potential role in acid/base catalysis, which was validated using the $EanB_{Y353A}$ and $EanB_{Y353F}$ variants. Even under single-turnover conditions, for both variants, ergothioneine production is below the ^{1}H-NMR detection limit and < 0.3% according to quantitative mass spectrometry analysis (**Figure S11a-c**). Upon co-crystallizing of $EanB_{Y353A}$ with polysulfide and

hercynine, two more states were observed (**Table S1**): i) The EanB$_{Y353A}$•hercynine•trisulfide tetrahedral intermediate (**Figure 4b**); and ii) the EanB$_{Y353A}$•ergothioneine binary complex with the Cys412 persulfide (**Figure 4c**). In EanB$_{Y353A}$, the Tyr355's hydroxyl group moves closer to the hercynine's ε-carbon (4.0 Å), partially filling the space occupied by Tyr353 in EanB$_{WT}$. In addition, Cys412 is in a trisulfide form in the EanB$_{Y353A}$ mutant, instead of a persulfide in EanB$_{WT}$, possibly due to additional space created by mutating Tyr353 to a smaller Ala residue (**Figure 4b** & **Figure S10b**). More importantly, the trisulfide directly links to the hercynine's ε-carbon in a tetrahedral conformation and we propose that this state is the captured C-S bond containing tetrahedral intermediate. We also observed the EanB$_{Y353A}$•ergothioneine binary complex with the Cys412 persulfide (**Figure 4c** & **Figure S10c**). We attribute this result to the very low level of activity in this mutant and in the two-week crystallization process, some of the tetrahedral intermediate formed in **Figure 4b** proceeded to the product.

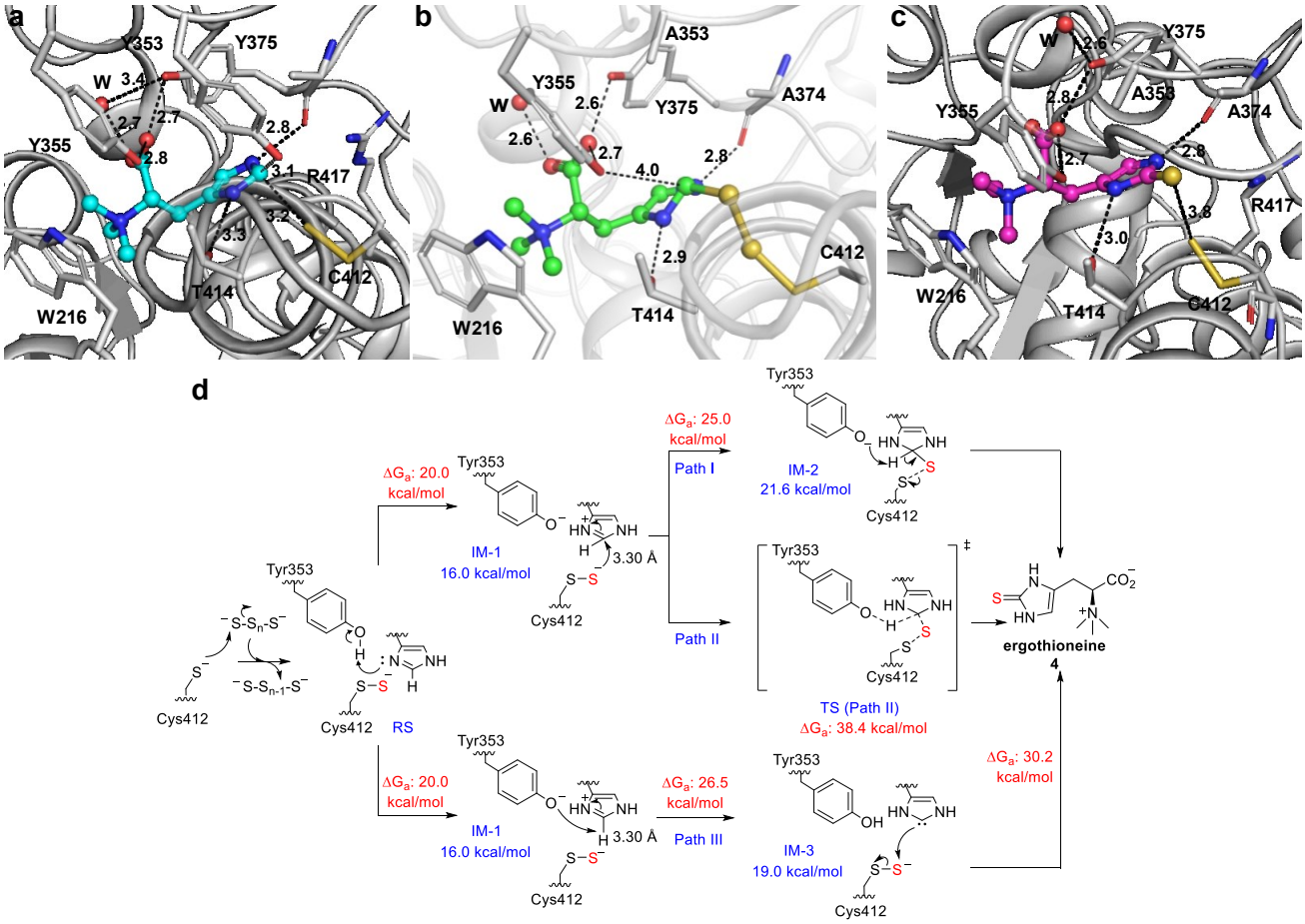

Figure 4. Crystal structures of three states in EanB-catalysis and our EanB-mechanistic models based on the QM/MM calculation. (**a**)-(**c**) Catalytic states of EanB observed in crystallographic studies. (**a**) The EanB•hercynine binary complex with the Cys412 persulfide intermediate. Hercynine is shown in cyan sticks and key interactions are shown in dash lines with distances labeled (in Å). (**b**) EanB$_{Y353A}$•hercynine•Cys412-trisulfide in the tetrahedral intermediate state (shown in green sticks). (**c**) The EanB$_{Y353A}$•ergothioneine binary complex (ergothioneine shown in a magenta sticks). (**d**) Proposed mechanisms for EanB-catalysis based on the QM/MM calculation. After the protonation of hercynine's imidazole ring N$_\pi$, C-S bond formation is followed by the deprotonation of Tyr353 (Path I) or a concerted mechanism in which the C-S bond is formed simultaneously with the transfer of H$^+$ to the deprotonated Tyr353 (Path II). Path III shows the deprotonation of the protonated imidazole by Tyr353 to a carbene intermediate (IM-3), which is then followed by the C-S bond formation.

The activation of an unreactive C-H bond in EanB-catalysis. With the structural information, the next question we examined is: how is the unreactive C-H bond of hercynine activated to accept the sulfur atom from EanB's Cys412 persulfide? We analyzed this reaction using metadynamics free energy

simulations and efficient hybrid quantum mechanics/molecular mechanic methods (QM/MM). Our starting point is the crystal structure the pre-reaction state (**Figure 4a**). The computed free energy surfaces (**Figure S12**) suggest that the initial step in the reaction involves the proton transfer from Tyr353 to the hercynine's N_π atom (**Figure 4d**). The role of Tyr353 for hercynine's N_π atom is also supported by a hydrogen bonding analysis from the EanB•hercynine binary complex with the Cys412 persulfide crystal structure (**Figure S9f-g**). The energetics of model reactions with different protonation states of substrate analogs support the proposal that protonation of hercynine is required for the nucleophilic persulfide attack (**Figure S16** and **Supporting discussion**). The two-dimensional free energy surface in **Figure S12b-c** further supports this hypothesis, showing that the energetically favorable pathway starts from hercynine's N_π protonation by Tyr353, leading to a metastable intermediate IM-1; by contrast, sulfur transfer without this protonation is energetically uphill without any free energy basin that corresponds to a well-defined intermediate. In the EanB pre-reaction state (**Figure 4a**), the Thr414 and the hercynine's N_π atom participate in H-bonding (**Figure S14**). Specifically, the Thr414 plays a key role in orienting hercynine for productive proton transfer and in stabilizing the deprotonated Tyr353. IM-1 is ~16.0 kcal•mol^{-1} above the reactant state (RS) and this step (RS $\rightarrow$ IM-1, **Figure 4d**) has a free energy barrier (ΔG_a) of ~20.0 kcal•mol^{-1}. Once IM-1 is formed, nucleophilic attack by the Cys412 persulfide leads to C-S bond formation, resulting in the tetrahedral intermediate IM-2 at the hercynine's ε-carbon, which is ~21.6 kcal•mol^{-1} relative to the reactant state; the activation free energy barrier is ~25.0 kcal•mol^{-1} measured relative to the reactant. We created the $EanB_{Y353A}$, $EanB_{Y353F}$, and $EanB_{T414V}$ variants. Even under single-turnover conditions, their ergothioneine production is below the ^{1}H-NMR detection limit and < 0.3% according to quantitative mass spectrometry analysis (**Figure S11a-d**). These biochemical results are consistent with the proposed key roles of these residues in EanB-catalysis. Starting from IM-1 or IM-2, the sulfur transfer and the proton transfer back to Tyr353 may occur via one of several pathways as outlined in **Figure 4d** and **Supporting discussion**. Path II has a much higher activation energy than Path I. In path III, after the hercynine's imidazole is protonated by Tyr353, the deprotonated Tyr353 then deprotonates hercynine at the ε-position to produce a carbene intermediate. The fact that S-S bond cleavage has higher activation free energy in all three pathways suggests that proton transfer reactions are not rate-limiting steps, in agreement with the solvent and substrate KIE data.[16] These QM/MM studies suggest that the protonation of hercynine's imidazole side-chain by Tyr353 is the key activation step that initiates the S-S bond cleavage in EanB-catalysis.

▪ DISCUSSION AND CONCLUSIONS

Despite the significance of sulfur-containing molecules in nature, many of their biosynthetic pathways are poorly understood.[1-6] In literature, there are two types of C-S bond formation mechanisms: ionic and radical; and several reviews summarize the current knowledge on enzymatic C-S bond formation reactions.[2,5,6,41] Recently, the biosynthetic information of a few more excellent examples of sulfur-containing natural products have been described. One of these interesting classes of transformations is the conversion of amides to thioamides via the ionic type of reaction mechanism. Specifically, in the 6-thioguanine biosynthesis, YcfA (a ATP-dependent sulfur-transferase) and YcfC (a cysteine desulfurase) catalyze thioamide formation.[42] Recently, the closthiamide's biosynthetic gene cluster has been identified and the biosynthetic pathway has been partially reconstituted in *E. coli*.[43] Results from these genetic studies imply that the thioamide formation in closthiamide biosynthesis may follow a mechanism similar to that in 6-thioguanine's biosynthesis. However, the sulfur source and the closthiamide biosynthetic details remain to be characterized. In contrast, the thioamidation of the α-subunit of methyl-coenzyme M reductase (McrA) by an ATP-dependent sulfur-transferase YcaO, is slightly different.[44] In YcaO-catalysis, sulfide is the direct sulfur source. Another recent example from the biosynthesis of sulfur-containing natural products is the installation of oxazolone and thioamide to produce methanobactin from its precursor peptide. This reaction is catalyzed by the MbnB/MbnC herterodimer, wherein the MbnB contains a non-heme iron active site. The Installation of oxazolone and thioamide in the MbnB/MbnC reaction is proposed to involve radical intermediates.[45]

Among these biosynthetic pathways for sulfur-containing natural products, ergothioneine biosyntheses are unique because both aerobic and anaerobic biosynthetic pathways have been discovered.[6,14,15,17] One of the key feature for the C-S bond formation is the replacement of an unactivated sp^2 C-H bond by a C-S bond, which is a difficult chemical transformation (i.e., energetically unfavorable). In the aerobic ergothioneine biosynthetic pathways from *M. smegmatis*[14] and *N. crassa*[15] (Figure 1a), non-heme iron enzymes (EgtB or Egt1, Figure

1a) catalyze the sp^2 C-H bond activation. EgtB/Egt1-catalyzed reactions are four-electron oxidation processes with molecular oxygen as the oxidant. Interestingly, in the anaerobic ergothioneine biosynthetic pathway from the green-sulfur bacterium *C. limicola,* a rhodanese (EanB, Figure 1a) directly replaces the sp^2 C-H bond by a C-S bond. Rhodaneses perform key roles in the biosyntheses of sulfur-containing cofactors (e.g., thiamine or molybdenum cofactor), and in thiolation of nucleic acids.[46] In these systems, thiocarboxylates (R-CO-SH) or protein-bound cysteine persulfides (R-S-SH) are the sulfur donors, resulting in persulfide-bound rhodaneses. Additionally, a complicated sulfur-transfer relay pathway provides the sulfur atom from cysteine, thiosulfate, or mercaptopyruvate.[20,46] The persulfide' s sulfur of these rhodaneses then attacks electrophilic carbons such as those on the phosphorylated C-terminus of sulfur carrier proteins or phosphorylated nucleobases to afford a covalent enzyme-substrate complex. A second active site cysteine then cleaves the disulfide bond, resulting in the thiolate product. Unlike the other literature examples of rhodaneses, the trans-sulfuration reaction of EanB is unique in at least two aspects: 1) small molecular polysulfide is the direct sulfur source; and, 2) the hercynine's ε-carbon sp^2 C-H bond is not activated for C-S bond formation.

Our biochemical results indicate that the small molecular polysulfide is the direct sulfur source for EanB-catalysis in ergothioneine biosynthesis. Pentasulfide has been observed in the crystal structure of a Radical SAM enzyme (MiaB).[47] However, it is generally believed that the iron-sulfur cluster attached sulfide/polysulfide is the substrate in MiaB catalysis.[47,48] Notably, sulfide does not support EanB-catalysis. Therefore, EanB is the first reported case of an enzyme using polysulfide as the direct sulfur source in a natural product biosynthesis. Recent characterization of sulfur granules deposited in sulfur bacteria revealed that there are various forms of polysulfides, including S8, polysulfide, cysteine polysulfide, and glutathione polysulfide.[21-23] In sulfur-based respiration, green sulfur bacteria utilize sulfide as the electron source and in these sulfur-oxidizing pathways, polysulfides are key intermediates.[49] In sulfur bacteria, flavocytochrome c (FCC) and sulfide:quinone oxioreductase (SQR) are the primary enzymes for the oxidation of sulfide to produce polysulfide.[35,50] A second system for polysulfide production is the degradation of cysteine and cystine by cystathionine β-lyase.[35] This reaction leads to cysteine persulfide as the product. However, cysteine persulfide can disproportionate to produce polysulfide, which is the key reaction for producing polysulfide in mammalian systems. This reaction is also present in bacteria. Mutation of SQR led to a growth defect when the mutant was cultured under high sulfide concentrations.[51] Given by the abundance of different polysulfides deposited in green sulfur bacteria,[23] and the ability of EanB to utilize these sulfur donors, it is tempting to propose that the trans-sulfuration reaction mediated by EanB is an example demonstrating the link between sulfur-related energy metabolism and the biosynthesis of secondary metabolites in green sulfur bacteria. Our discovery warrants further investigation of this link.

The structural studies also provide another line of evidence supporting the use of small-molecule polysulfides as the direct sulfur donor in EanB-catalysis. The EanB active site's cysteine (Cys412) is deeply buried within the protein, and, therefore, not accessible by the protein-bound thiocarboxylates or persulfide intermediates present in these previously reported sulfur-transfer relay systems. In contrast, a small molecular polysulfide is able to access this deep tunnel and act as the direct sulfur source for the EanB reaction. Moreover, structural studies coupled with the QM/MM analysis also provide valuable insights into the mechanism of C-H bond activation mediated by EanB. The computational studies highlight the importance of the protonation of hercynine's N_π atom by Tyr353 for nucleophilic persulfide attack. After the imidazole's side-chain is activated, the reaction may proceed to produce a C-S bond via either a sequential (Path I) or concerted (Path II) mechanism (**Figure 4d**). Alternatively, the C-S bond can be formed via a carbene intermediate (Path III, **Figure 4d**). Intriguingly, the carbene pathway was proposed in previous studies and deemed unlikely.[16,17] The crystallographic observation of a tetrahedral intermediate in the $EanB_{Y353A}$ variant implies that most likely, pathway I (i.e., the nucleophilic attack of the persulfide on the protonated hercynine) is in operation (**Figure 4d**). From our QM/MM analysis, the ΔG_a for the sequential pathway (Path I) is ~25.0 kcal•mol^{-1}, very close to that of the carbene-involved reaction (Path III, **Figure 4d**), suggesting that the carbene pathway may not be ruled out yet. Carbene intermediates have been proposed in thiamine diphosphate dependent enzymes,[52] and orotidine 5′-phosphate decarboxylase.[53]

Overall, our study illuminates the use of polysulfide as the direct sulfur source for EanB-catalysis in the biosynthesis of an emerging longevity vitamin, ergothioneine. Since polysulfides are the *in vivo* sul-

fur forms in green sulfur bacteria, EanB-catalysis also exemplifies how the biosyntheses of sulfur-containing secondary metabolites are coupled with bacteria physiology and sulfur-related energy metabolism.[49,54,55] EanB homologs are found in many other sulfur bacteria, suggesting that other similar biosynthetic pathways await to be unveiled.[17,56]

▪ EXPERIMENTAL SECTION

Materials: Reagents were purchased from Sigma-Aldrich and Fisher Scientific unless otherwise specified. Hercynine was synthesized following reported procedure.[57] Proton and carbon nuclear magnetic resonance spectra were recorded using Agilent 500 (500 MHz VNMRS). The kinetic parameter was determined using Cary Bio-100 spectrophotometer (Agilent).

Protein overexpression and purification. EanB gene (accession number ACD90218.1) was codon-optimized for *Escherichia coli* overexpression by Genscript and sub-cloned into pET28a-(+) vector. *E.coli* BL21(DE3) was transformed with the EanB-pET28a plasmid and a single colony was inoculated into 50 mL LB media supplemented with 50 μg•mL^{-1} kanamycin at 37 °C overnight. Then, 10-mL of seed culture was used to inoculate 1 L of LB media supplemented with 50 μg•mL^{-1} kanamycin at 37 °C. When OD_{600nm} reached 0.6-0.8, protein overexpression was induced with 0.2 mM isopropyl β-D-1-thiogalactopyranoside (IPTG) final concentration at 16 °C. The culture was supplemented with potassium phosphate (KPi) buffer pH 7.0 to 100 mM final concentration. After additional 12 hr, the cells were harvest by centrifugation.

The EanB purification was carried out under anaerobic environment (see **Supporting Methods**). The purified protein concentration was quantified by amino acid analysis (AAA Service Lab). The extinction coefficient of the purified protein is 85815±1460 M^{-1}cm^{-1} based amino acid analysis (correction factor based on concentration determined from Bradford analysis is 0.735).

The mutant constructs were generated using Q5 Site-directed Mutagenesis Kit following suggested protocol (New England Biolabs). The overexpression and purification of the variants were carried out following the protocol of the wild type EanB. Notably, due to the instability of $EanB_{C412\text{-only}}$ mutant, the lysis buffer for the purification of this mutant was changed to 100 mM Tris-HCl, 500 mM NaCl, and 10% glycerol, pH 8.0.

IscS gene (accession number YP_026169.1) was amplified from *E. coli* with forward primer 5'-GAGAGAATTCAAATTACCGATTTATCTCGACTACTCCG-3' and reverse primer 5'-GAGACTCGAGATGATGAGCCCATTCGATGCTGTT-3' (The EcoRI and XhoI digestion were indicated with underline). The gene was sub-cloned into pET28a-(+) vector. *E.coli* BL21(DE3) was transformed with the plasmid. The IscS protein was overexpressed using a protocol similar to that of EanB except that PLP was added as a supplement to 0.1 mM final concentration. Moreover, after addition of IPTG, cells were incubated at 16 °C for 8 hours before harvest by centrifugation. IscS was purified following protocol similar to that of EanB (see **Supporting Methods**).

The DNA sequence of *Burkholderia sp. HME13* ergothionase (accession number BAM63550.1)[32] was synthesized by Genscript, codon optimized for *Escherichia coli* overexpression. The synthetic gene was sub-cloned into pET28a-(+) vector. The ergothionase protein was overexpressed using a protocol similar to that of EanB. After induction by IPTG, cells were incubated at 16 °C for 12 hours before harvesting by centrifugation. Ergothionase was purified by following a protocol similar to that of EanB (see **Supporting Methods**).

^{1}H NMR analysis of EanB activity. The EanB-IscS was conducted anaerobically. A 1-mL reaction contained 2 μM EanB, 1 mM hercynine, 1 mM cysteine, and 4 μM IscS, in 50 mM KPi pH 8.0 buffer at room temperature for 8 hours. The reaction was lyophilized and analyzed by ^{1}H NMR. To determine the sulfur source in EanB-catalysis, several potential sulfur donors were examined. A 1-mL reaction mixture containing 2 μM EanB, 1 mM hercynine, 1 mM of varous potential sulfur donors (K_2S_x, S_8, S_8 with DTT, $Na_2S_2O_3$, NaHS, mercaptopyruvate, S_8 with cysteine, and S_8 with GSH) in 50 mM pH 8.0 KPi buffer for 8 hours. The reaction was lyophilized and ergothioneine formation was analyzed using ^{1}H NMR assay. All ^{1}H-NMR spectra were calibrated by the water peak at 4.65 ppm.

EanB-ergothionase coupled assay with IscS. An EanB continuous activity assay was developed by converting ergothioneine to thiolurocanic acid using ergothionase (HME13) from *Burkholderia sp.*[32] The reaction was monitored at 311 nm ($\varepsilon_{311nm} = 1.8 \times 10^5$ M^{-1}•cm^{-1}). A 1-mL reaction contained 2 μM IscS, 1 mM cysteine, 1 mM hercynine, 400 nM ergothionase (1000-fold of EanB activity), and various EanB concentration (2-10 μM) in 50 mM pH 8.0 KPi buffer at 25 °C. Specifically, the buffer, substrates, ergothionase, and IscS were added in order and mixed by stirring bar in the buffer for 10 seconds and the reaction was initiated by the addition of EanB. A control reaction containing all except ergothionase, was set up to serve as the control reaction for the baseline correction. The absorption from the control reaction was subtracted from that of the reaction to yield final reaction trace. Each reaction was repeated in triplicates and the activity measurement was repeated at least three more times.

Analysis of precipitate from EanB-IscS reaction mixture. To characterize the precipitates from the EanB-IscS reaction, a 1.2-mL reaction containing 2

μM EanB, 2 μM IscS, 1 mM hercynine, and 1 mM cysteine, was set up anaerobically in 50 mM pH 8.0KPi buffer. At hour 6 and hour 12, the precipitate was collected by centrifuging at 10,000 rpm for 1 min at 4 °C and washed to remove residual soluble protein using 1 mL of 50 mM KPi, pH 8.0. Then, the precipitate was resuspended in 20 μL of 100 mM Na_2S solution and incubated at room temperature for 0.5 h. Subsequently, the sample was diluted with MeOH to 0.2 mL final volume and derivatized with 20 μL of methyl triflate. The dimethylated species were subjected to HPLC analysis (90% MeOH, 10% H_2O, 0.5 mL•min^{-1}) using C18 column (4.6 × 250 mm, 5 μm, YMC-triart) with 10 μL injection volume.

In addition to sulfur-based analysis, the precipitates were analyzed by SDS-PAGE to visualize protein in the samples. At the beginning of the reaction, the concentration of protein was quantified to be ~0.35 mg•mL^{-1}. At hour 6 and hour 12, the precipitate was collected by centrifuging at 10,000 rpm for 1 min at 4 °C and resuspended in 30 μL of SDS-loading dye. A 100-μL aliquot of the supernatant was taken and diluted with 100 μL SDS-loading dye and 10 μL of each sample was loaded for SDS-PAGE analysis. Accounting for the dilution factor of SDS-PAGE sample preparation, the proteins in precipitates at hour 6 and hour 12 were quantified as ~2 μg and ~4 μg by SDS-PAGE quantification with in-house protein standard, which represented only 1% and 2% of total soluble protein in supernatant, respectively.

Steady-state kinetic analysis of EanB reaction with polysulfides. The kinetic parameters of EanB-catalysis were determined using EanB-ergothionase coupled assay. For hercynine concentration dependent study, a 1-mL reaction contained 1.8 μM EanB, 400 nM ergothionase (1000-fold of EanB activity), 0.116 mM K_2S_x, and varying concentration of hercynine (0.01 – 1 mM) in 50 mM KPi buffer, pH 8.0 at 25°C. Buffer, substrates and ergothionase were added in order and mixed by stir bar for 2 min to equilibrate the polysulfide disproportionation reaction in buffer so as to confirm there is no background absorbance from polysulfide disproportionation reaction and trace among of protein. The reaction was initiated by the addition of EanB. The baseline correction was performed following the EanB-IscS ergothionase assay. The reaction was monitored at 311 nm. Each reaction was repeated in triplicates. For polysulfide concentration dependent study, a 1-mL reaction mixture containing 1.8 μM EanB, 400 nM ergothionase (1000-fold of EanB activity), 0.5 mM hercynine, and varying concentration of K_2S_x (6 - 289 μM) in 50 mM KPi buffer, pH 8.0 was set up at 25°C. Each reaction was repeated in triplicates and the data was fitted by GraphPad Prism. Polysulfide is a mixture of S_3^{2-} to S_9^{2-} species, while the dominant species of polysulfide under our assay condition was determined as S_4^{2-} (see **Supporting Methods**). The reported K_M was calculated using concentration of S_4^{2-}.

Similar to the wild type, the kinetic parameters of $EanB_{C412\text{-only}}$ was characterized using ergothionase coupled assay. For hercynine concentration dependent study, a 1-mL reaction contained 7.6 μM EanB, 400 nM ergothionase (1000-fold of EanB activity), 0.116 mM K_2S_x, and varying concentration of hercynine (0.02 – 2 mM) in 50 mM KPi buffer, pH 8.0 at 25°C. For polysulfide concentration dependent study, a 1-mL reaction mixture containing 7.6 μM EanB, 400 nM ergothionase (1000-fold of EanB activity), 0.5 mM hercynine, and varying concentration of K_2S_x (6 - 289 μM) in 50 mM KPi buffer, pH 8.0 was set up at 25 °C. Each reaction was repeated in triplicates.

Protein crystallization. Crystals of the wild-type of EanB were grown at 18 °C in anaerobic box, using the sitting-drop vapor diffusion method in 2 μL drops, containing 1:1 mixture of 10 mg•mL^{-1} protein solution (in 25 mM Tris-HCl, pH8.0, 150 mM NaCl) and the reservoir consisting of 0.1 M MOPS/HEPES, pH 7.5, 0.03 M of each ethylene glycol, 10% PEG 20k, 20% PEG 550 MME. Needle-like crystals were observed after two weeks. EanB•hercynine binary complex was crystallized at 20 °C using sitting drop vapor diffusion method under aerobic condition. Purified EanB protein was incubated with 1 mM hercynine solved in water on ice for 30 min. 1 μL of this protein-substrate mixture was mixed with 1 μL reservoir and the complex crystals appeared after one week in the condition of 0.1 M MES/imidazole pH 6.5, 0.02 M of each alcohol, 10% PEG20k, 20% PEG 550 MME. All EanB-hercynine-polysulfide complex were crystallized using sitting drop vapor diffusion method at 18 °C in anaerobic box. The purified EanB proteins were incubated with 1 mM hercynine (prepared in water) and 2 mM potassium polysulfide (prepared in water) for 30 min and followed by centrifugation, mixing in a 1:1 ratio with the reservoir solution in a final volume of 2 μL.

The complex crystals of EanB•ergothioneine intermediate were grown in 0.1 M Bis-Tris pH 6.5, 28% PEG 2000MME. The complex crystals of $EanB_{Y353A}$•ergothioneine with Cys412 in its persulfide form were grown in 0.1 M imidazole/MES buffer system, pH 6.5, 0.09 M halogens (NaF, NaBr, NaI), 30% mix 1 (PEG500MME_PEG20k). The crystals of $EanB_{Y353A}$•ergothioneine tetrahedral intermediate were grown in condition of 0.1 M imidazole, sodium cacodylate, MES, Bis-Tris, pH 6.5, 0.09 M halogens (NaF,NaBr,NaI), 37.5% MPD_P1k_PEG3350. All crystals were flash-frozen in liquid nitrogen after being dipped into a solution containing 10-15% glycerol or only reservoir.

Data collection and structures determination. The diffraction data of *apo* EanB was collected at the wavelength of 0.97918 Å on SSRF beamline SSRF-

BL18U1 Shanghai (China). The data of EanB with hercynine, EanB with hercynine and polysulfide complex were collected at the wavelength of 0.97930 Å on SSRF beamline SSRF-BL18U1 Shanghai (China). The complex data of $EanB_{Y353A}$ with hercynine and polysulfide was collected at the wavelength of 0.97791 Å on SSRF beamline SSRF-BL19U1 Shanghai (China). All data collection was performed at 100 K. All data, collected on SSRF-BL18U1 and 19U1, sets were indexed, integrated, and scaled using the HKL3000 package,[58] collected on SSRF-BL17U1, sets were indexed, integrated, and scaled using the HKL2000 package.[59] The structures of *apo* EanB were solved by molecular replacement method using the program PHASER[60] and the structure of 3IPP as the search model, rounds of automated refinement were performed with PHENIX[61] and the models were extended and rebuilt manually with COOT,[62] the structure have been refined to 2.17 Å. The complex structure of EanB with hercynine, with hercynine and polysulfide, mutant EanB with hercynine and polysulfide were solved by the same method and using *apo* EanB structure as the search model. The statistics for data collection and crystallographic refinement are summarized in **Table S1**.

$EanB_{C412\text{-}only}$-IscS single-turnover reaction. The following experiment was conducted under anaerobic environment unless noted otherwise. For IscS single-turnover reaction, a 2-mL reaction containing 1.3 mM IscS and 1.2 mM [β-^{13}C]-cysteine (0.9-fold of IscS) in 100 mM Tris-HCl, pH 8.0, was set up at room temperature for 5 min. A 400-µL portion was taken and quench by HCl. Precipitated protein was removed by centrifugation. The supernatant was neutralized with NH_4HCO_3 and analyzed by ^{13}C NMR to ensure the formation of protein-bound persulfide of IscS by checking the formation of [β-^{13}C]-alanine. Then, excess cysteine in the remaining portion was removed by G25 size-exclusion chromatography (30 mm × 600 mm) at 4 °C. Then, a portion of cysteine-treated IscS was then alkylated in a 200-µL reaction containing 0.22 mM cysteine-treated IscS and 2.6 mM iodoacetamide in 100 mM Tris-HCl, 200 mM NaCl, pH 8.0 for 1 hour and the mixture was shielded from light.

After confirming the activity of IscS, $EanB_{C412\text{-}only}$ was incubated with the remaining portion of cysteine-treated IscS in a 1: 1 ratio at 155 µM final concentration in 4.5-mL reaction of 100 mM Tris-HCl, 200 mM NaCl, pH 8.0. Then, a 200-µL alkylation reaction containing 100 µM cysteine-treated IscS, 100 µM $EanB_{C412\text{-}only}$, and 1.6 mM iodoacetamide in 100 mM Tris-HCl, 200 mM NaCl, pH 8.0 for 1 hour. The remaining of $EanB_{C412\text{-}only}$-IscS was used for single-turnover reaction. A 4.2-mL reaction containing 155 µM $EanB_{C412\text{-}only}$, 155 µM IscS, and 775 µM hercynine (5-fold of EanB) in 100 mM Tris-HCl, 200 mM NaCl, pH 8.0, was set up for 15 min. Then, a 200-µL alkylation reaction was set up as previously described prior to hercynine addition. A 500-µL aliquot of reaction mixture was taken and mixed with 100 µL 6 M HCl. The protein precipitates were removed by centrifugation and the supernatant was taken for ergothioneine quantification by mass spectrometry. Additionally, the activity of IscS after size exclusion column was confirmed through multiple-turnover assay, which contained 10 µM $EanB_{C412\text{-}only}$, 1 mM hercynine, 1 mM cysteine, 4 µM IscS in 50 mM KPi, pH 8.0 for 8 hr. The reaction was lyophilized and analyzed ^{1}H NMR assay. Additionally, to determine the production of ergothioneine from persulfide of as-purified protein, a 50-µL reaction containing 396 µM $EanB_{C412\text{-}only}$ and 1.98 mM hercynine in 100 mM Tris-HCl, 200 mM NaCl, pH 8.0, was set up for 15 min. Then, the ergothioneine formation was quantified using mass spectrometry. This experiment was repeated twice. The figures presented here are representative of the results from this experiment.[34]

$EanB_{C412\text{-}only}$-polysulfide single-turnover reaction. This study was carried out following that of wild type EanB reaction. The experiment was performed anaerobically. An alkylation reaction of as-purified $EanB_{C412\text{-}only}$ was set up. This 100-µL reaction containing 0.2 mM $EanB_{C412\text{-}only}$ and 0.8 mM iodoacetamide in 150 mM Tris-HCl, pH 8.0, was set up at room temperature shielded from light for 1 hour. Then, a 2.7-mL reaction containing 353 µM $EanB_{C412\text{-}only}$ and 5.3 mM K_2S_x in 150 mM Tris-HCl, pH 8.0, was set up at room temperature for 5 min. Then, excess polysulfides were removed using G-25 size-exclusion chromatography. The fractions containing protein were pooled. Then, a 120-µL alkylation reaction containing 65 µM K_2S_x-treated $EanB_{C412\text{-}only}$ and 260 µM iodoacetamide in 150 mM Tris-HCl, pH 8.0, was set up at room temperature for 1 hour and the mixture was shielded from light. Then, a 7.2-mL reaction containing 65 µM K_2S_x-treated $EanB_{C412\text{-}only}$ and 325 µM hercynine (5-fold of enzyme) in 150 mM Tris-HCl, pH 8.0 at room temperature for 15 min. A 120-µL reaction containing 65 µM $EanB_{C412\text{-}only}$ and 260 µM of iodoacetamide as described previously. The alkylated samples were used for tandem mass spectrometry analysis as discussed previously. A 500-µL aliquot of reaction mixture was taken and mixed with 100 µL of 6 M HCl. The protein precipitates were removed by centrifugation and the supernatant was taken for ergothioneine quantification by mass spectrometry (See **Supporting Methods**). Additionally, the activity of $EanB_{C412\text{-}only}$ was confirmed through multiple-turnover assay, which contained 10 µM K_2S_x-treated $EanB_{C412\text{-}only}$, 1 mM hercynine, 1 mM K_2S_x, in 50 mM KPi, pH 8.0 for 8 hours. The reaction was lyophilized and analyzed by ^{1}H NMR spectroscopy. Additionally, to determine the production of ergothioneine from persulfide of as-purified protein, a 50-µL reaction containing 396 µM $EanB_{C412\text{-}only}$ and 1.98 mM hercynine in 100 mM Tris-HCl, 200 mM NaCl, pH 8.0, was set up for 15 min. Then, the ergothioneine formation was quantified using mass spec-

trometry. The persulfide content of EanB after treated with polysulfide was determined through cyanolysis assay (see **Supporting Methods**). This experiment was then repeated twice. The figures presented here are representative of the results from this experiment.

Computational Methods. All simulations were performed using CHARMM[63]. The crystal structure of EanB in complex with hercynine and Cys412 polysulfide was used. Hydrogens were added to the structure by using the HBUILD module of CHARMM. A 25 Å spherical water droplet centered on the terminal sulfur atom of Cys412 persulfide was added to solvate the enzyme system. Non-crystallographic waters within 2.5 Å of any crystallographic atom were deleted. The system was separated into three regions following the QM/MM-GSBP protocol (**Figure S12**)[64,65]: a QM region with the active site treated with an efficient quantum mechanical method at the DFTB3 level of theory[64,66,67], along with the 3OB-3-1 parameters.[68,69] The QM region consisted of 134 atoms, including key reacting residues, the hercynine substrate and some residues in α-helix 18 (i.e. Glu345, Tyr353, Tyr411, Cys412, Gly413, Thr414, Gly415, Trp416, Arg417 and Gly418). QM link atoms, using the DIV scheme[70], were placed between the alpha and beta carbons of QM residues. No water molecules were included in the QM region. Non-QM atoms within a 28 Å sphere surrounding the active site (7961 atoms) were treated with the CHARMM36 force field[71,72]. Water molecules were described with a modified TIP3P model[73]. All atoms (1971 atoms) outside of the 28 Å sphere were frozen. The inner sphere was treated with classical Newtonian dynamics, except for a buffer region of 3 Å thickness from the edge of the sphere, which was treated with Langevin dynamics. Protein atoms in the buffer region were harmonically constrained with force constants determined from the average of crystallographic B factors.[74] After a short geometry optimization, the system was heated from 48 K and equilibrated at 298 K over the course of 100 ps. Then, the system was further equilibrated at 298 K for 250 ps.

Possible catalytic mechanisms were explored with metadynamics simulations[75,76] using the PLUMED package[77] interfaced to CHARMM. The collective variables (CVs) for metadynamics were the antisymmetric stretch involving proton transfers between Tyr353 and the hercynine substrate (N for the first step, and ε-C for the subsequent steps), and the antisymmetric stretch that describes the nucleophilic attack of sulfur to ε-carbon of the substrate. In the simulation, SHAKE[78] was applied to bonds involving hydrogens that do not participate in proton transfer. The multiple walker metadynamics method was utilized with typically 500 walkers per simulation. Gaussian potentials were placed every 100 fs; the Gaussian height was set to be 0.25 kcal•mol^{-1}, and the Gaussian width for the antisymmetric stretch was set as 0.1 Å. The convergence was examined by monitoring the free energy of key species as a function of the number of Gaussians included (**Figure S13**); representative snapshots for these key species are included in **Figure S14** and **S15**. The two-dimensional potential of mean force PMF shown in **Figure S12** is based on a metadynamics simulation with 500 walkers. The corresponding simulation was performed for 50 ns (100 ps for each walker). and 100 ns (200 ps for each walker) for **Figure S12b** and **S12c**, respectively. The similar QM/MM methodology has been successfully applied to a number of enzyme systems in recent studies.[79-81]

To evaluate the accuracy of DFTB3 for the reactions of interest here, several small model systems were used as shown in **Figure S16**. All QM calculations for these model systems were performed using the Gaussian 16 program[82]. Single point energy calculations at DFTB3 minimized structures were performed using the Becke, three-parameter, Lee-Yang-Parr exchange-correlation functional (B3LYP)[83] with the addition of Grimme's third version semi-empirical dispersion correction (D3)[84]. The 6-31G(d,p) basis set[85,86] and 6-311++G(d,p) basis set[87,88] were used in the calculation. In addition, the G3B3 method[89] was used in proton affinity calculations. Due to significant errors in proton affinity, the C-H repulsive potential in DFTB3/3OB was reparametrized based on electronic energies obtained at the MP2/aug-cc-pVQZ level of theory,[90-92] as shown in Table S2. To further confirm the exothermicity of the reaction and the stability of possible intermediates, geometry optimizations were also performed with conductor-like polarizable continuum solvation model[93,94] (dielectric constant as 4.0 to model the solvation effect of the protein environment) by using a truncated model based on QM/MM calculations (136 atoms, as shown in **Figure S16c**). In addition, the potential energy surface (PES) for carbene and persulfide reaction was examined both at DFTB3 and B3LYP-D3/6-311++G(d,p) levels of theory (as shown in **Figure S17**).

▪ AUTHOR INFORMATION

Corresponding Authors

Pinghua Liu — [1]*Department of Chemistry, Boston University, Boston, MA 02215, USA*; Email: Pinghua@bu.edu

Jiahai Zhou — [2]*State Key Laboratory of Bio-organic and Natural Products Chemistry, Center for Excellence in Molecular Synthesis, Shanghai Institute of Organic Chemistry, University of Chinese Academy of Sciences, Shanghai 200032, China;* Email: jiahai@mail.sioc.ac.cn

Qiang Cui — [1]*Department of Chemistry, Boston University, Boston, MA 02215, USA*; Email: qiangcui@bu.edu

Authors

Ronghai Cheng — [1]*Department of Chemistry, Boston University, Boston, MA 02215, USA*.

Lian Wu — [2]*State Key Laboratory of Bio-organic and Natural Products Chemistry, Center for Excellence in Molecular Synthesis, Shanghai Institute of Organic Chemistry, University of Chinese Academy of Sciences, Shanghai 200032, China;* [8]*Key Laboratory of Synthetic Biology, CAS Center for Excellence in Molecular Plant Sciences, Institute of Plant Physiology and Ecology, Shanghai Institutes for Biological Sciences, Shanghai 200032, China;* [9]*College of Life Science, University of Chinese Academy of Sciences, Beijing 100049, China*.
Rui Lai — [1]*Department of Chemistry, Boston University, Boston, MA 02215, USA*.
Chao Peng — [3]*National Facility for Protein Science in Shanghai, Zhangjiang Lab, Shanghai Advanced Research Institute, Chinese Academy of Science, Shanghai 201210, China*.
Nathchar Naowarojna — [1]*Department of Chemistry, Boston University, Boston, MA 02215, USA*.
Weiyao Hu — [1]*Department of Chemistry, Boston University, Boston, MA 02215, USA;* [4]*School of Chemistry and Chemical Engineering, Shanghai Jiao Tong University, Shanghai, 200240, China*.
Xinhao Li — [4]*School of Chemistry and Chemical Engineering, Shanghai Jiao Tong University, Shanghai, 200240, China*.
Stephen A. Whelan — [1]*Department of Chemistry, Boston University, Boston, MA 02215, USA*.
Norman Lee — [1]*Department of Chemistry, Boston University, Boston, MA 02215, USA*.
Juan Lopez — [1]*Department of Chemistry, Boston University, Boston, MA 02215, USA*.
Changming Zhao — [1]*Department of Chemistry, Boston University, Boston, MA 02215, USA;* [5]*Key Laboratory of Combinatory Biosynthesis and Drug Discovery (Wuhan University), Ministry of Education, School of Pharmaceutical Sciences, Wuhan University, Hubei 430072, People's Republic of China*.
Youhua Yong — [2]*State Key Laboratory of Bio-organic and Natural Products Chemistry, Center for Excellence in Molecular Synthesis, Shanghai Institute of Organic Chemistry, University of Chinese Academy of Sciences, Shanghai 200032, China*.
Jiahui Xue — [6]*Shanghai Key Laboratory of Green Chemistry and Chemical Process, East China Normal University, 3663 North Zhongshan Road, Shanghai 200062, P. R. China*.
Xuefeng Jiang — [6]*Shanghai Key Laboratory of Green Chemistry and Chemical Process, East China Normal University, 3663 North Zhongshan Road, Shanghai 200062, P. R. China*.
Mark W. Grinstaff — [1]*Department of Chemistry, Boston University, Boston, MA 02215, USA;* [7]*Department of Biomedical Engineering, Boston University, Boston, MA 02215, USA*. *0000-0002-5453-3668*
Zixin Deng — [5]*Key Laboratory of Combinatory Biosynthesis and Drug Discovery (Wuhan University), Ministry of Education, School of Pharmaceutical Sciences, Wuhan University, Hubei 430072, People's Republic of China*.
Jiesheng Chen — [4]*School of Chemistry and Chemical Engineering, Shanghai Jiao Tong University, Shanghai, 200240, China*.

Author Contributions

†Ronghai Cheng, Lian Wu, Rui Lai, Chao Peng, and Nathchar Naowarojna contributed equally to this work.

Notes

The authors declare no competing financial interest.

▪ ASSOCIATED CONTENT

Supporting Information

More detailed experimental procedures, protein purification and characterization, additional structural information and expanded discussion of our computation work are included in the Supporting information. This information is available free of charge on the ACS Publications website.

▪ ACKNOWLEDGMENT

This work is partially supported by the MOST (2019YFA09005000 and 2018YFA0901900), CAS (XDB20000000) and SMSTC (19XD1404800) (J.Z.), the National Science Foundation (CHE-2004109) and National Institute of Health (AT010878 to P.L. and GM-106443 to Q. C.), National Natural Science Foundation of China project (31500667, C.P.) and the Chinese Academy of Science Key Technology Talent Program to C.P. We thank Zhihong Li and Chen Su of the Mass Spectrometry System at the National Facility for Protein Science in Shanghai (NFPS), Zhangjiang Lab, SARI, China for providing technical support and assistance in data collection and analysis. The authors thank the staff of beamlines BL18U1 and BL19U1 of Shanghai Synchrotron Radiation Facility for access and help with the X-ray data collection. The authors also thank P. Li and J. Gan for help with data collection and structure refinement, and Profs. Sean Elliott and Deborah Perlstein for feedback on the manuscript.

▪ REFERENCES

(1) Fontecave, M.; Ollagnier-de-Choudens, S.; Mulliez, E., Biological radical sulfur insertion reactions. *Chem. Rev.* **2003**, *103*, 2149-66.
(2) Lin, C. I.; McCarty, R. M.; Liu, H. W., The biosynthesis of nitrogen-, sulfur-, and high-carbon chain-containing sugars. *Chem. Soc. Rev.* **2013**, *42*, 4377-407.
(3) Kessler, D., Enzymatic activation of sulfur for incorporation into biomolecules in prokaryotes. *FEMS Microbiol. Rev.* **2006**, *30*, 825-840.
(4) Mueller, E. G., Trafficking in persulfides: delivering sulfur in biosynthetic pathways. *Nat. Chem. Biol.* **2006**, *2*, 185-194.
(5) Dunbar, K. L.; Scharf, D. H.; Litomska, A.; Hertweck, C., Enzymatic carbon-sulfur bond formation in natural product biosynthesis. *Chem. Rev.* **2017**, *117*, 5521-5577.
(6) Naowarojna, N.; Cheng, R.; Chen, L.; Quill, M.; Xu, M.; Zhao, C.; Liu, P., Mini-review: ergothioneine and ovothiol biosyntheses, an unprecedented trans-sulfur strategy in natural product biosynthesis. *Biochemistry* **2018**, *57*, 3309-3325.
(7) Fahey, R. C., Novel thiols of prokaryotes. *Annu. Rev. Microbiol.* **2001**, *55*, 333-356.
(8) Cheah, I. K.; Halliwell, B., Ergothioneine; antioxidant potential, physiological function and role in disease. *Biochim. Biophys. Acta, Mol. Basis Dis.* **2012**, *1822*, 784-793.
(9) Grundemann, D.; Harlfinger, S.; Golz, S.; Geerts, A.; Lazar, A.; Berkels, R.; Jung, N.; Rubbert, A.; Schomig, E., Discovery of the ergothioneine transporter. *Proc. Natl. Acad. Sci. U.S.A.* **2005**, *102*, 5256-61.
(10) Ames, B. N., Prolonging healthy aging: longevity vitamins and proteins. *Proc. Natl. Acad. Sci. U.S.A.* **2018**, *115*, 10836-10844.
(11) Davies, H. M. L.; Du Bois, J.; Yu, J. Q., C-H functionalization in organic synthesis. *Chem. Soc. Rev.* **2011**, *40*, 1855-1856.
(12) Gutekunst, W. R.; Baran, P. S., C-H functionalization logic in total synthesis. *Chem. Soc. Rev.* **2011**, *40*, 1976-1991.
(13) Yamaguchi, J.; Yamaguchi, A. D.; Itami, K., C-H bond functionalization: emerging synthetic tools for natural products and pharmaceuticals. *Angew. Chem. Int. Ed.* **2012**, *51*, 8960-9009.
(14) Seebeck, F. P., *In vitro* reconstitution of mycobacterial ergothioneine biosynthesis. *J. Am. Chem. Soc.* **2010**, *132*, 6632-6633.

(15) Hu, W.; Song, H.; Her, A. S.; Bak, D. W.; Naowarojna, N.; Elliott, S. J.; Qin, L.; Chen, X. P.; Liu, P. H., Bioinformatic and biochemical characterizations of C-S bond formation and cleavage enzymes in the fungus *Neurospora crassa* ergothioneine biosynthetic pathway. *Org. Lett.* **2014**, *16*, 5382-5385.
(16) Leisinger, F.; Burn, R.; Meury, M.; Lukat, P.; Seebeck, F. P., Structural and mechanistic basis for anaerobic ergothioneine biosynthesis. *J. Am. Chem. Soc.* **2019**, *141*, 6906-6914.
(17) Burn, R.; Misson, L.; Meury, M.; Seebeck, F. P., Anaerobic origin of ergothioneine. *Angew. Chem. Int. Ed.* **2017**, *56*, 12508-12511.
(18) Cipollone, R.; Ascenzi, P.; Visca, P., Common themes and variations in the rhodanese superfamily. *IUBMB Life* **2007**, *59*, 51-59.
(19) Jurgenson, C. T.; Begley, T. P.; Ealick, S. E., The structural and biochemical foundations of thiamin biosynthesis. *Annu. Rev. Biochem.* **2009**, *78*, 569-603.
(20) Sasaki, E.; Zhang, X.; Sun, H. G.; Lu, M. Y. J.; Liu, T. L.; Ou, A.; Li, J. Y.; Chen, Y. H.; Ealick, S. E.; Liu, H. W., Co-opting sulphur-carrier proteins from primary metabolic pathways for 2-thiosugar biosynthesis. *Nature* **2014**, *510*, 427-431.
(21) Gregersen, L. H.; Bryant, D. A.; Frigaard, N.-U., Mechanisms and evolution of oxidative sulfur metabolism in green sulfur bacteria. *Front. Microbiol.* **2011**, *2*, 1-14.
(22) Frigaard, N.-U.; Dahl, C., Sulfur metabolism in phototrophic sulfur bacteria. *Adv. Microb. Physiol.* **2008**, *54*, 103-200.
(23) Prange, A.; Chauvistre, R.; Modrow, H.; Hormes, J.; Truper, H. G.; Dahl, C., Quantitative speciation of sulfur in bacterial sulfur globules: X-ray absorption spectroscopy reveals at least three different species of sulfur. *Microbiology* **2002**, *148*, 267-276.
(24) Mihara, H.; Esaki, N., Bacterial cysteine desulfurases: their function and mechanisms. *Appl. Microbiol. Biotechnol.* **2002**, *60*, 12-23.
(25) Selbach, B.; Earles, E.; Dos Santos, P. C., Kinetic Analysis of the Bisubstrate Cysteine Desulfurase SufS from Bacillus subtilis. *Biochemistry* **2010**, *49*, 8794-8802.
(26) Albrecht, A. G.; Netz, D. J. A.; Miethke, M.; Pierik, A. J.; Burghaus, O.; Peuckert, F.; Lill, R.; Marahiel, M. A., SufU Is an Essential Iron-Sulfur Cluster Scaffold Protein in Bacillus subtilis. *J. Bacteriol.* **2010**, *192*, 1643-1651.
(27) Loiseau, L.; Ollagnier-de Choudens, S.; Lascoux, D.; Forest, E.; Fontecave, M.; Barras, F., Analysis of the Heteromeric CsdA-CsdE Cysteine Desulfurase, Assisting Fe-S Cluster Biogenesis in Escherichia coli. *J. Biol. Chem.* **2005**, *280*, 26760-26769.
(28) Lauhon, C. T.; Kambampati, R., The iscS Gene in Escherichia coli Is Required for the Biosynthesis of 4-Thiouridine, Thiamin, and NAD. *J. Biol. Chem.* **2000**, *275*, 20096-20103.
(29) Zheng, L.; Cash, V. L.; Flint, D. H.; Dean, D. R., Assembly of Iron-Sulfur Clusters: identification of an iscSUA-hscBA-fdx gene cluster from Azotobacter Vinelandii. *J. Biol. Chem.* **1998**, *273*, 13264-13272.
(30) Hidese, R.; Mihara, H.; Esaki, N., Bacterial cysteine desulfurases: versatile key players in biosynthetic pathways of sulfur-containing biofactors. *Appl. Microbiol. Biotechnol.* **2011**, *91*, 47-61.
(31) Kelley, L. A.; Mezulis, S.; Yates, C. M.; Wass, M. N.; Sternberg, M. J. E., The Phyre2 web portal for protein modeling, prediction and analysis. *Nat. Protoc.* **2015**, *10*, 845-858.
(32) Muramatsu, H.; Matsuo, H.; Okada, N.; Ueda, M.; Yamamoto, H.; Kato, S.-i.; Nagata, S., Characterization of ergothionase from Burkholderia sp. HME13 and its application to enzymatic quantification of ergothioneine. *Appl. Microbiol. Biotechnol.* **2013**, *97*, 5389-5400.
(33) Black, K. A.; Dos Santos, P. C., Shared-intermediates in the biosynthesis of thio-cofactors: mechanism and functions of cysteine desulfurases and sulfur acceptors. *Biochim. Biophys. Acta, Mol. Cell. Res.* **2015**, *1853*, 1470-1480.
(34) Zheng, L. M.; White, R. H.; Cash, V. L.; Jack, R. F.; Dean, D. R., Cysteine desulfurase activity indicates a role for NIFS in metallocluster biosynthesis. *Proc. Natl. Acad. Sci. U.S.A.* **1993**, *90*, 2754-2758.
(35) Filipovic, M. R.; Zivanovic, J.; Alvarez, B.; Banerjee, R., Chemical biology of H_2S signaling through persulfidation. *Chem. Rev.* **2018**, *118*, 1253-1337.
(36) Kamyshny, A.; Goifman, A.; Gun, J.; Rizkov, D.; Lev, O., Equilibrium distribution of polysulfide ions in aqueous solutions at 25 °C: a new approach for the study of polysulfides equilibria. *Environ. Sci. Technol.* **2004**, *38*, 6633-6644.
(37) Wood, J. L., Sulfane sulfur. *Methods Enzymol.* **1987**, *143*, 25-29.
(38) Kharma, A.; Grman, M.; Misak, A.; Dominguez-Alvarez, E.; Nasim, M. J.; Ondrias, K.; Chovanec, M.; Jacob, C., Inorganic polysulfides and related reactive sulfur-selenium species from the perspective of chemistry. *Molecules* **2019**, *24*, 1-15.
(39) Bhasin, M.; Garg, A.; Raghava, G. P., PSLpred: prediction of subcellular localization of bacterial proteins. *Bioinformatics* **2005**, *21*, 2522-4.
(40) Yu, C. S.; Chen, Y. C.; Lu, C. H.; Hwang, J. K., Prediction of protein subcellular localization. *Proteins Struct. Funct. Bioinf.* **2006**, *64*, 643-651.
(41) Burkhart, B. J.; Schwalen, C. J.; Mann, G.; Naismith, J. H.; Mitchell, D. A., YcaO-dependent posttranslational amide activation: biosynthesis, structure, and function. *Chem. Rev.* **2017**, *117*, 5389-5456.
(42) Litomska, A.; Ishida, K.; Dunbar, K. L.; Boettger, M.; Coyne, S.; Hertweck, C., Enzymatic thioamide formation in a bacterial antimetabolite pathway. *Angew. Chem. Int. Ed.* **2018**, *57*, 11574-11578.
(43) Dunbar, K. L.; Büttner, H.; Molloy, E. M.; Dell, M.; Kumpfmüller, J.; Hertweck, C., Genome editing reveals novel thiotemplated assembly of polythioamide antibiotics in anaerobic bacteria. *Angew. Chem. Int. Ed.* **2018**, *130*, 14276-14280.
(44) Dong, S.-H.; Liu, A.; Mahanta, N.; Mitchell, D. A.; Nair, S. K., Mechanistic basis for ribosomal peptide backbone modifications. *ACS Cent. Sci.* **2019**, *5*, 842-851.
(45) Kenney, G. E.; Dassama, L. M.; Pandelia, M.-E.; Gizzi, A. S.; Martinie, R. J.; Gao, P.; DeHart, C. J.; Schachner, L. F.; Skinner, O. S.; Ro, S. Y., The biosynthesis of methanobactin. *Science* **2018**, *359*, 1411-1416.
(46) Wright, C. M.; Christman, G. D.; Snellinger, A. M.; Johnston, M. V.; Mueller, E. G., Direct evidence for enzyme persulfide and disulfide intermediates during 4-thiouridine biosynthesis. *Chem. Commun.* **2006**, 3104-3106.
(47) Forouhar, F.; Arragain, S.; Atta, M.; Gambarelli, S.; Mouesca, J. M.; Hussain, M.; Xiao, R.; Kieffer-Jaquinod, S.; Seetharaman, J.; Acton, T. B.; Montelione, G. T.; Mulliez, E.; Hunt, J. F.; Fontecave, M., Two Fe-S clusters catalyze sulfur insertion by radical-SAM methylthiotransferases. *Nat. Chem. Biol.* **2013**, *9*, 333-338.
(48) Landgraf, B. J.; Arcinas, A. J.; Lee, K. H.; Booker, S. J., Identification of an intermediate methyl carrier in the radical *S*-adenosylmethionine methylthiotransferases RimO and MiaB. *J. Am. Chem. Soc.* **2013**, *135*, 15404-15416.
(49) Findlay, A. J., Microbial impact on polysulfide dynamics in the environment. *FEMS Microbiol. Lett.* **2016**, *363*, 1-12.
(50) Griesbeck, C.; Hauska, G.; Schütz, M., Biological sulfide oxidation: sulfide-quinone reductase (SQR), the primary reaction. *Recent Res. Devel. Microbiology* **2000**, *4*, 179-203.
(51) Chan, L.-K.; Morgan-Kiss, R. M.; Hanson, T. E., Functional analysis of three sulfide: quinone oxidoreductase homologs in Chlorobaculum tepidum. *J. Bacteriol.* **2009**, *191*, 1026-1034.
(52) Meyer, D.; Neumann, P.; Ficner, R.; Tittmann, K., Observation of a stable carbene at the active site of a thiamin enzyme. *Nat. Chem. Biol.* **2013**, *9*, 488-490.
(53) Miller, B. G.; Wolfenden, R., Catalytic proficiency: the unusual case of OMP decarboxylase. *Annu. Rev. Biochem.* **2002**, *71*, 847-885.
(54) Falkenby, L. G.; Szymanska, M.; Holkenbrink, C.; Habicht, K. S.; Andersen, J. S.; Miller, M.; Frigaard, N. U., Quantitative proteomics of *Chlorobaculum tepidum*: insights into the sulfur metabolism of a phototrophic green sulfur bacterium. *FEMS Microbiol. Lett.* **2011**, *323*, 142-150.
(55) Jormakka, M.; Yokoyama, K.; Yano, T.; Tamakoshi, M.; Akimoto, S.; Shimamura, T.; Curmi, P.; Iwata, S., Molecular mechanism of energy conservation in polysulfide respiration. *Nat. Struct. Mol. Biol.* **2008**, *15*, 730-737.
(56) Ruszczycky, M. W.; Liu, H. W., The surprising history of an antioxidant. *Nature* **2017**, *551*, 37-38.
(57) Song, H.; Leninger, M.; Lee, N.; Liu, P., Regioselectivity of the oxidative C–S bond formation in ergothioneine and ovothiol biosyntheses. *Org. Lett.* **2013**, *15*, 4854-4857.
(58) Minor, W.; Cymborowski, M.; Otwinowski, Z.; Chruszcz, M., HKL-3000: the integration of data reduction and structure solution - from diffraction images to an initial model in minutes. *Acta Crystallogr., Sect. D: Biol. Crystallogr.* **2006**, *62*, 859-866.
(59) Otwinowski, Z.; Minor, W., Processing of X-ray diffraction data collected in oscillation mode. *Methods Enzymol.* **1997**, *276*, 307–326.
(60) McCoy, A. J.; Grosse-Kunstleve, R. W.; Adams, P. D.; Winn, M. D.; Storoni, L. C.; Read, R. J., Phaser crystallographic software. *J. Appl. Crystallogr.* **2007**, *40*, 658-674.
(61) Adams, P. D.; Afonine, P. V.; Bunkóczi, G.; Chen, V. B.; Davis, I. W.; Echols, N.; Headd, J. J.; Hung, L.-W.; Kapral, G. J.; Grosse-Kunstleve, R.

W., PHENIX: a comprehensive Python-based system for macromolecular structure solution. *Acta Crystallogr., Sect. D: Biol. Crystallogr.* **2010**, *66*, 213-221.
(62) Emsley, P.; Cowtan, K., Coot: model-building tools for molecular graphics. *Acta Crystallogr., Sect. D: Biol. Crystallogr.* **2004**, *60*, 2126-2132.
(63) Brooks, B. R.; Brooks III, C. L.; Mackerell Jr, A. D.; Nilsson, L.; Petrella, R. J.; Roux, B.; Won, Y.; Archontis, G.; Bartels, C.; Boresch, S., CHARMM: the biomolecular simulation program. *J. Comput. Chem.* **2009**, *30*, 1545-1614.
(64) Cui, Q.; Elstner, M.; Kaxiras, E.; Frauenheim, T.; Karplus, M., A QM/MM implementation of the self-consistent charge density functional tight binding (SCC-DFTB) method. *J. Phys. Chem. B* **2001**, *105*, 569-585.
(65) Schaefer, P.; Riccardi, D.; Cui, Q., Reliable treatment of electrostatics in combined QM/MM simulation of macromolecules. *Chem. Phys.* **2005**, *123*, 014905.
(66) Elstner, M.; Porezag, D.; Jungnickel, G.; Elsner, J.; Haugk, M.; Frauenheim, T.; Suhai, S.; Seifert, G., Self-consistent-charge density-functional tight-binding method for simulations of complex materials properties. *Phys. Rev. B: Condens. Matter* **1998**, *58*, 7260-7268.
(67) Gaus, M.; Cui, Q.; Elstner, M., DFTB3: extension of the self-consistent-charge density-functional tight-binding method (SCC-DFTB). *J. Chem. Theory Comput.* **2011**, *7*, 931-948.
(68) Gaus, M.; Lu, X.; Elstner, M.; Cui, Q., Parameterization of DFTB3/3OB for sulfur and phosphorus for chemical and biological applications. *J. Chem. Theory Comput.* **2014**, *10*, 1518-1537.
(69) Lu, X.; Gaus, M.; Elstner, M.; Cui, Q., Parametrization of DFTB3/3OB for magnesium and zinc for chemical and biological applications. *J. Phys. Chem. B* **2014**, *119*, 1062-1082.
(70) König, P.; Hoffmann, M.; Frauenheim, T.; Cui, Q., A critical evaluation of different QM/MM frontier treatments with SCC-DFTB as the QM method. *J. Phys. Chem. B* **2005**, *109*, 9082-9095.
(71) Mackerell Jr, A. D.; Feig, M.; Brooks III, C. L., Extending the treatment of backbone energetics in protein force fields: limitations of gas‐phase quantum mechanics in reproducing protein conformational distributions in molecular dynamics simulations. *J. Comput. Chem.* **2004**, *25*, 1400-1415.
(72) MacKerell Jr, A. D.; Bashford, D.; Bellott, M.; Dunbrack Jr, R. L.; Evanseck, J. D.; Field, M. J.; Fischer, S.; Gao, J.; Guo, H.; Ha, S., All-atom empirical potential for molecular modeling and dynamics studies of proteins. *J. Phys. Chem. B* **1998**, *102*, 3586-3616.
(73) Jorgensen, W. L.; Chandrasekhar, J.; Madura, J. D.; Impey, R. W.; Klein, M. L., Comparison of simple potential functions for simulating liquid water. *J. Chem. Phys.* **1983**, *79*, 926-935.
(74) Brooks III, C. L.; Karplus, M., Solvent effects on protein motion and protein effects on solvent motion: dynamics of the active site region of lysozyme. *J. Mol. Biol.* **1989**, *208*, 159-181.
(75) Laio, A.; Gervasio, F. L., Metadynamics: a method to simulate rare events and reconstruct the free energy in biophysics, chemistry and material science. *Rep. Prog. Phys.* **2008**, *71*, 126601.
(76) Laio, A.; Parrinello, M., Escaping free-energy minima. *Proc. Natl. Acad. Sci. U.S.A.* **2002**, *99*, 12562-12566.
(77) Bonomi, M.; Branduardi, D.; Bussi, G.; Camilloni, C.; Provasi, D.; Raiteri, P.; Donadio, D.; Marinelli, F.; Pietrucci, F.; Broglia, R. A., PLUMED: a portable plugin for free-energy calculations with molecular dynamics. *Comput. Phys. Commun.* **2009**, *180*, 1961-1972.
(78) Ryckaert, J.-P.; Ciccotti, G.; Berendsen, H. J., Numerical integration of the cartesian equations of motion of a system with constraints: molecular dynamics of n-alkanes. *J. Comput. Phys.* **1977**, *23*, 327-341.
(79) Roston, D.; Demapan, D.; Cui, Q., Leaving Group Ability Observably Affects Transition State Structure in a Single Enzyme Active Site. *J. Am. Chem. Soc.* **2016**, *138*, 7386-7394.
(80) Roston, D.; Cui, Q., Substrate and transition state binding in alkaline phosphatase analyzed by computation of oxygen isotope effects. *J. Am. Chem. Soc.* **2016**, *138*, 11946-11957.
(81) Roston, D.; Demapan, D.; Cui, Q., Extensive free-energy simulations identify water as the base in nucleotide addition by DNA polymerase. *Proc. Natl. Acad. Sci. U.S.A.* **2019**, *116*, 25048-25056.
(82) Gaussian 16, Frisch, M. J.; Trucks, G. W.; Schlegel, H. B.; Scuseria, G. E.; Robb, M. A.; Cheeseman, J. R.; Scalmani, G.; Barone, V.; Petersson, G. A.; Nakatsuji, H.; Li, X.; Caricato, M.; Marenich, A. V.; Bloino, J.; Janesko, B. G.; Gomperts, R.; Mennucci, B.; Hratchian, H. P.; Ortiz, J. V.; Izmaylov, A. F.; Sonnenberg, J. L.; Williams; Ding, F.; Lipparini, F.; Egidi, F.; Goings, J.; Peng, B.; Petrone, A.; Henderson, T.; Ranasinghe, D.; Zakrzewski, V. G.; Gao, J.; Rega, N.; Zheng, G.; Liang, W.; Hada, M.; Ehara, M.; Toyota, K.; Fukuda, R.; Hasegawa, J.; Ishida, M.; Nakajima, T.; Honda, Y.; Kitao, O.; Nakai, H.; Vreven, T.; Throssell, K.; Montgomery Jr., J. A.; Peralta, J. E.; Ogliaro, F.; Bearpark, M. J.; Heyd, J. J.; Brothers, E. N.; Kudin, K. N.; Staroverov, V. N.; Keith, T. A.; Kobayashi, R.; Normand, J.; Raghavachari, K.; Rendell, A. P.; Burant, J. C.; Iyengar, S. S.; Tomasi, J.; Cossi, M.; Millam, J. M.; Klene, M.; Adamo, C.; Cammi, R.; Ochterski, J. W.; Martin, R. L.; Morokuma, K.; Farkas, O.; Foresman, J. B.; Fox, D. J. Gaussian, Inc., Wallingford, CT, 2016
(83) Becke, A., Density‐functional thermochemistry. III. The role of exact exchange. *J. Chem. Phys.* **1993**, *98*, 5648-5652.
(84) Grimme, S.; Antony, J.; Ehrlich, S.; Krieg, H., A consistent and accurate ab initio parametrization of density functional dispersion correction (DFT-D) for the 94 elements H-Pu. *J. Chem. Phys.* **2010**, *132*, 154104.
(85) Hehre, W. J.; Ditchfield, R.; Pople, J. A., Self‐consistent molecular orbital methods. XII. Further extensions of Gaussian−type basis sets for use in molecular orbital studies of organic molecules. *J. Chem. Phys.* **1972**, *56*, 2257-2261.
(86) Francl, M. M.; Pietro, W. J.; Hehre, W. J.; Binkley, J. S.; Gordon, M. S.; DeFrees, D. J.; Pople, J. A., Self‐consistent molecular orbital methods. XXIII. A polarization‐type basis set for second‐row elements. *J. Chem. Phys.* **1982**, *77*, 3654-3665.
(87) Clark, T.; Chandrasekhar, J.; Spitznagel, G. W.; Schleyer, P. V. R., Efficient diffuse function‐augmented basis sets for anion calculations. III. The 3‐21+ G basis set for first‐row elements, Li‐F. *J. Comput. Chem.* **1983**, *4*, 294-301.
(88) Krishnan, R.; Binkley, J. S.; Seeger, R.; Pople, J. A., Self‐consistent molecular orbital methods. XX. A basis set for correlated wave functions. *J. Chem. Phys.* **1980**, *72*, 650-654.
(89) Baboul, A. G.; Curtiss, L. A.; Redfern, P. C.; Raghavachari, K., Gaussian-3 theory using density functional geometries and zero-point energies. *J. Chem. Phys.* **1999**, *110*, 7650-7657.
(90) Kendall, R. A.; Dunning Jr, T. H.; Harrison, R. J., Electron affinities of the first‐row atoms revisited. Systematic basis sets and wave functions. *J. Chem. Phys.* **1992**, *96*, 6796-6806.
(91) Physical reviewMøller, C.; Plesset, M. S., Note on an approximation treatment for many-electron systems. *Phys. Rev.* **1934**, *46*, 618.
(92) Dunning Jr, T. H., Gaussian basis sets for use in correlated molecular calculations. I. The atoms boron through neon and hydrogen. *J. Chem. Phys.* **1989**, *90*, 1007-1023.
(93) Barone, V.; Cossi, M., Quantum calculation of molecular energies and energy gradients in solution by a conductor solvent model. *J. Phys. Chem. A* **1998**, *102*, 1995-2001.
(94) Cossi, M.; Rega, N.; Scalmani, G.; Barone, V., Energies, structures, and electronic properties of molecules in solution with the C‐PCM solvation model. *J. Comput. Chem.* **2003**, *24*, 669-681.

Table of Contents